

THE EFFECT OF COBALT DOPING ON THE HEMATITE MATERIAL SYNTHESIZED USING PRECIPITATION METHOD AS A LITHIUM-ION BATTERY ANODE

L. Suyati; F.F.A. Rizky; S.S.L.A. Al-Zaitun; Gunawan; D.S. Widodo

Corresponding author's e-mail: linda_suyati@live.undip.ac.id

DOI: 10.47760/cognizance.2023.v03i11.031

ABSTRACT: Hematite is an iron oxide that has the most stable and environmentally friendly structure. Hematite is used as a good anode material, this is due to its high specific capacity, good chemical and thermal stability, and low cost. Hematite has weaknesses, namely poor cycle stability, unable to withstand volume changes, and low conductivity values. To improve the electrochemical performance of lithium-ion batteries, modifications are made to the anode material by adding a dopant. This research aims to synthesize Co-doped hematite material with variations of 0.2, 4, and 6.8% using NaOH and KOH precipitating agents, characterize Co-doped hematite material using FTIR, XRD, SEM-EDX, and analyze its electrochemical performance as a lithium-ion battery anode. The method used is deposition. The synthesis results obtained brick red and black precipitates. FTIR characterization shows that the sample contains the Fe-O-Fe functional group which appears at wave numbers 519.19 and 517.32 cm^{-1} . Based on XRD characterization, samples of undoped hematite and 6% Co had crystal sizes of 26.4193 nm and 20.6927 nm. SEM characterization results show that the morphology of the 6% Co-doped hematite sample has an irregular semi-spherical shape. The electrochemical test results show that the battery with the best electrochemical performance was produced by a 6% Co-doped hematite sample which had a conductivity value of 2.35×10^{-3} S/cm and the resulting battery capacity efficiency reached 99.9%.

Keywords: Hematite, cobalt, precipitation, anode, lithium-ion battery

INTRODUCTION

Technological developments over time have caused the intensity of the use of electronic devices such as laptops, smartphones, and other equipment to increase. This phenomenon then drives an increase in the need for the use of batteries, namely devices used to store electrical energy efficiently [1,2]. Li-ion batteries are non-disposable batteries with electrochemical reactions that occur back and forth [3]. Li-ion batteries have a long cycle life, low discharge power when not in use, high energy density, and are environmentally friendly [4]. Hematite (α - Fe_2O_3) is an iron oxide that has the most stable and environmentally friendly structure. Previously, researchers had conducted a synthesis of hematite anode materials and materials doped with Co using various methods. Fouad *et al.* [5] who have successfully synthesized the α - Fe_2O_3 material by applying the precipitation method using varying concentrations of the precursor $\text{Fe}_2(\text{SO}_4)_3 \cdot x\text{H}_2\text{O}$. Lassoued *et al.* [6] synthesized hematite using the precipitation method with variations in precipitating bases. Nithyadharseni *et al.* [7] synthesized SnO_2

nanomaterials doped with Zn, Co, and Mg metals for application in lithium-ion batteries, Co-SnO₂ nanomaterials produced the best electrochemical performance, namely showing the lowest resistance and the largest specific capacity reaching 575 mAh/g after 50 cycles with Capacity retention is approximately 83%. Hematite is used as a good anode material, this is due to its high specific capacity, conductivity value of 5.2×10^{-3} S/cm, good chemical and thermal stability, and low cost. Hematite has the disadvantages of poor cycle stability, unable to withstand volume changes, and low conductivity values [8,9]. To improve the electrochemical performance of lithium-ion batteries, modifications were made to the anode material by applying Co doping which has an electrical conductivity of 1.79×10^7 S/cm [10]. Therefore, in this research, a Co-doped hematite material synthesis process will be carried out using NaOH and KOH precipitating agents which will be applied as anodes in lithium-ion batteries.

EXPERIMENTAL

Materials

The materials used are iron (III) nitrate pentahydrate [Fe(NO₃)₃.9H₂O] (PA), cobalt (II) nitrate hexahydrate [Co(NO₃)₂.6H₂O] (PA), deionized water (PA), sodium hydroxide [NaOH] (PA), potassium hydroxide [KOH] (PA), and filter paper.

Equipment

The equipment in this research was Erlenmeyer, graduated cylinder, iron spatula, analytical balance, beaker, burette, magnetic stirrer, thermometer, stirrer, funnel, porcelain crucible, watch glass, furnace, oven, vial, digital pH meter and universal pH paper, FTIR Spectroscopy (Perkin-Elmer UATR), XRD (Shimadzu).

Synthesis of Co-doping Hematite

The synthesis procedure in this research was carried out following the procedure used by Fouad *et al* [5] and Mansour *et al* [11] by modifying the precursor using Co-doping. First, preparation of 5 solutions of Fe(NO₃)₃ with a concentration of 0.45 M in 100 mL of deionized water To each solution was added a 0.45 M Co(NO₃)₂ solution with variations in the addition of 0, 2, 4, 6, and 8%. The solution was homogenized and heated to a temperature of 70⁰C with a magnetic stirrer for 20 minutes. Then, the addition of 3 M KOH to the solution dropwise until it reaches pH 11 and heat to reach a temperature of 85-90⁰C while stirring for 90 minutes. Next, the resulting precipitate was separated using filter paper and washed with deionized water several times. Then dried using an oven at a temperature of 100⁰C for 24 hours and the sample was calcined at a temperature of 700⁰C for 4 hours. The same procedure was repeated using the precipitating agent NaOH.

Characterization of Co-doped Hematite

The synthesis results obtained were characterized using FTIR, XRD, and SEM-EDX instruments. FTIR characterization is used to identify the presence of certain functional groups in samples. XRD characterization is used to identify the type of mineral, size and crystal structure, and crystallinity of the solid samples that have been synthesized. SEM-EDX is used to identify the surface morphology of particles, particle diameter, distribution, and composition of constituent elements contained in synthetic materials.

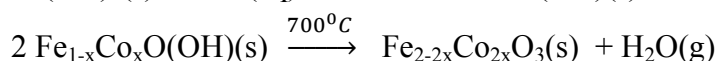
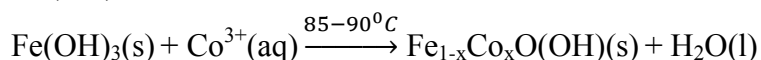
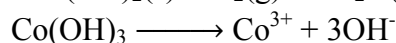
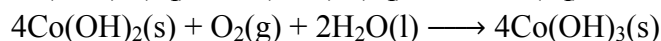
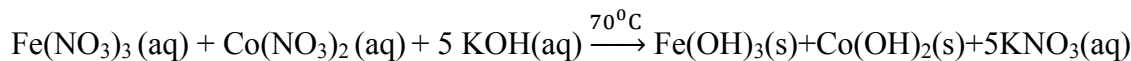
Co-Doped Hematite Electrochemical Activity Test on Lithium Ion Batteries

The activity test on the Co-doped hematite anode material in lithium-ion batteries was carried out using LCR testing. It was used to determine the amount of conductivity produced from the synthesized anode material and charge-discharge tests to provide information about the electrochemical performance of the battery. The information is in the form of its redox potential, current density, life cycle, and charge-discharge processes as well as analyzes the specific capacity that can be produced by the anode material in lithium-ion batteries.

RESULTS AND DISCUSSION

Synthesis Co-doped Hematite

The precipitate obtained from this synthesis process is in the form of brick red and black powder. The reaction mechanism according to [5,12,13] is as follows:



Characterization of Co Doped Hematite

Fourier Transform Infrared (FTIR) Spectroscopy Analysis

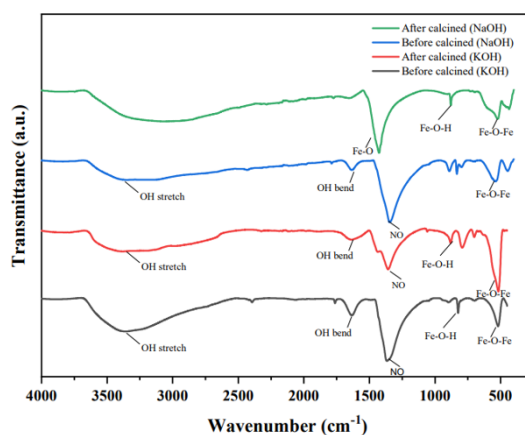


Figure 1. FTIR spectra before and after calcination of samples using NaOH and KOH precipitating agents

Based on the results, the sample before calcination obtained peaks as wave numbers of 3863.17 and 3342.10 cm^{-1} which indicated the stretching vibration of the O-H functional group, while the O-H bending vibration of the deionized water solvent was shown at a wave number of 1634.08 cm^{-1} . The peak that appears at 1367.32 cm^{-1} indicates the vibration of N=O. Wave

numbers of 895.26 cm^{-1} and 823.82 cm^{-1} indicate the presence of a functional group of Fe-O-H. The absorption peak at wave number 519.19 cm^{-1} indicates the presence of Fe-O-Fe. After calcination, O-H stretching vibrations and O-H bending vibrations from the deionized water solvent appears at wave numbers 3789.71 and 1636.54 cm^{-1} , respectively. Function group of N=O is at wave number 1359.01 cm^{-1} . The functional group of Fe-O-H appears at a wave number of 880.67 cm^{-1} and Fe-O-Fe appears at a wave number of 517.32 cm^{-1} .

X-Ray Diffraction Pattern

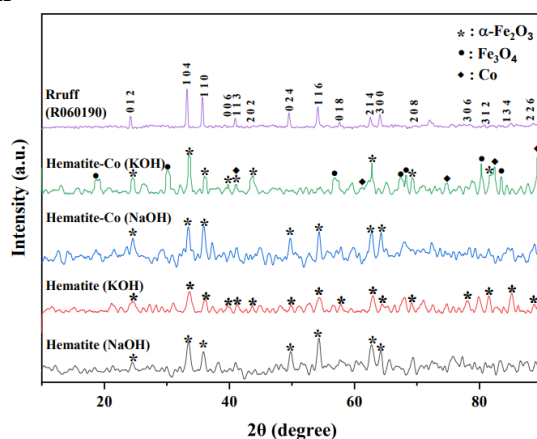


Figure 2. XRD spectra for hematite and hematite-Co (6%) samples

Based on XRD characterization, the hematite sample indicated the formation of a single phase in the form of hematite mineral which corresponds to the hematite diffraction pattern from the RRUFF database with ID: R060190, where the peak indicating the presence of the $\alpha\text{-Fe}_2\text{O}_3$ phase appears at 2θ : 24.68° ; 33.56° ; 35.96° ; 39.62° ; 41.18° ; 43.68° ; 49.78° ; 54.34° ; 57.80° ; 62.88° ; 64.32° ; 69.14° ; 77.98° ; 81.44° ; 85.22° ; 88.70° . These results were then strengthened by analysis using Match software with the Rietveld method to obtain hkl values for these peaks, namely (012), (104), (110), (006), (113), (202), (024), (116), (018), (214), (300), (208), (306), (312), (134), (226). In the hematite-Co sample, a phase other than $\alpha\text{-Fe}_2\text{O}_3$ was found, namely an impurity phase in the form of the Fe_3O_4 phase. The diffraction peak indicating the $\alpha\text{-Fe}_2\text{O}_3$ phase is shown at 2θ : 24.26° ; 33.24° ; 35.76° ; 39.56° ; 43.51° ; 62.87° ; 69.26° ; 81.34° , while 2θ is in position 18.50° ; 30.56° ; 57.75° ; 67.11° ; 80.28° ; 83.20° indicates the presence of the Fe_3O_4 phase. In addition, a cobalt phase was found which was characterized by the appearance of a diffraction peak at position 2θ : 40.79° ; 61.53° ; 74.55° ; 82.32° ; 89.06° . Meanwhile, in the samples using the precipitating agent NaOH, no other phases were found other than $\alpha\text{-Fe}_2\text{O}_3$. The success of Co-doping is characterized by a shift in the diffraction pattern, a change in the intensity of the diffraction peak, and a change in the width of the diffraction peak. The radius of the Co ion is smaller than the Fe ion, making it possible for the Co ion to be inserted into the crystal lattice so that it can replace the Fe ion [14]. The substitution of Fe^{3+} by Co^{3+} in the

goethite structure is carried out at the high pH of the aqueous solution of Fe^{3+} and Co^{2+} [12,15,16,17].

Scanning Electron Microscope- Energy Dispersive X-ray (SEM-EDX) Imaging

Based on the SEM-EDX results, it can be seen that the 4% Co-doped hematite sample in Figure 4(a) has a morphology that is not very homogeneous, there are still many small particles that stick to each other, forming agglomerations. This sample has an irregular semi-spherical particle shape with low density, while Figure 4(b) shows that the 6% Co-doped hematite sample has a morphology with a more homogeneous semi-spherical shape. The density in this sample is higher than with 6% doping.

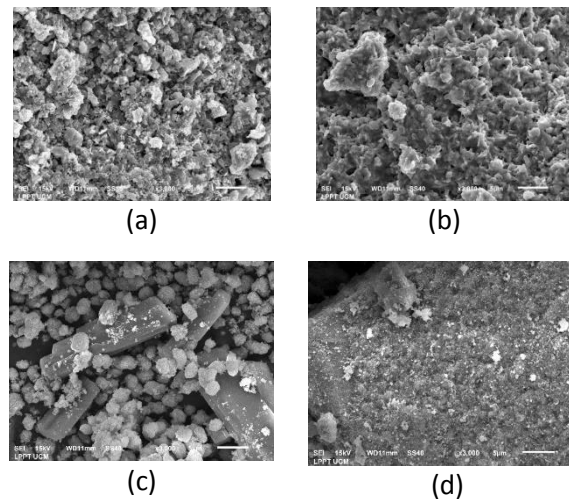
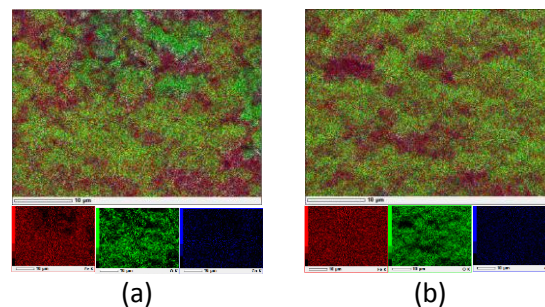


Figure 3. Surface morphology of Hematite-Co samples with KOH precipitating agent (a) 4% (b) 6% and Hematite-Co with NaOH precipitating agent (c) 4% (d) 6%



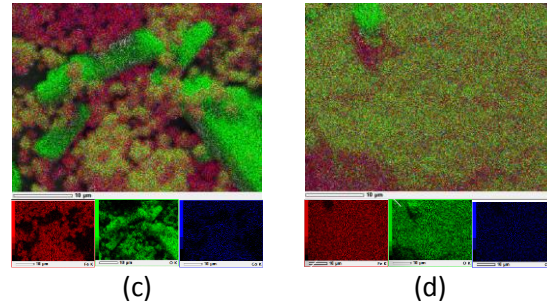


Figure 4. SEM-EDX Mapping of Hematite-Co samples with KOH precipitating agent (a) 4% (b) 6% and Hematite-Co with NaOH precipitating agent (c) 4% (d) 6%

This sample shows a more even distribution of elements, the distribution of the elements Fe and Co is much denser over the entire surface of the material. When compared with samples synthesized using the precipitating agent NaOH, KOH samples show a morphology and element distribution that is much more homogeneous and evenly distributed. The Co element in the 6% Co-doped sample has succeeded in replacing Fe atoms in hematite in greater amounts compared to the doped sample. cobalt as much as 4%. This is indicated by a decrease in the percentages of Fe atoms, the percentage which previously reached 36.71% decreased to 35.04%. Apart from that, it was also marked by an increase in the % Atom of Co from initially 1.19% to 1.53%. The element composition that is mostly contained in these two samples is the element of oxygen. This also proves that the sample that has been synthesized is hematite/Co, where oxygen is the element that contributes more to the structure of $Fe_{2-2x}Co_{2x}O_3$ compared to the element Fe. In the 4% Co doped sample, the percentage of oxygen atoms reached 62.10%, while in the 6% Co doped sample, the percentage of O atom was 63.43%.

LCR Analysis

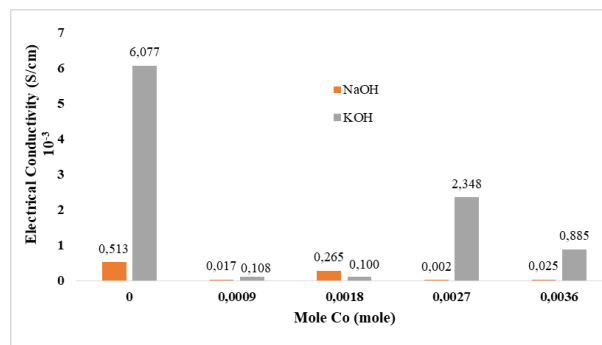


Figure 5. The relationship between LCR conductivity and variations in molar Co doped

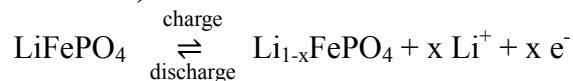
The highest conductivity value was obtained in the α - Fe_2O_3 sample synthesized using KOH with a value of 6.077×10^{-3} S/cm. After being given cobalt doping, the material showed a decrease in electrical conductivity to 2.348×10^{-3} S/cm resulting from the α - $Fe_{1.92}Co_{0.08}O_3$ sample, and the sample that produced the lowest conductivity was α - $Fe_{1.94}Co_{0.06}O_3$ of 0.100×10^{-3} S/cm.

³ S/cm. The sample synthesized using the deposition agent NaOH showed the highest conductivity value, namely that produced by the sample without doping of 0.513×10^{-3} S/cm. The electrical conductivity decreased after Co doping to 0.265×10^{-3} S/cm. Samples without Co doping have greater electrical conductivity compared to samples with Co doping, this is related to the distribution of elements and the morphology of the constituent particles. In samples with Co doping, the particle size is not very homogeneous, there are large and small particles. The small particles stick together, causing agglomeration. This agglomeration is one of the causes of hampered electrical conductivity. This is because when agglomeration occurs a resistive area will be formed which can inhibit and disrupt the movement of current [18]. Apart from that, the presence of the Fe₃O₄ phase is also one of the influencing factors for the decrease in the conductivity value of the material after Co doping is applied. This is because Fe₃O₄ is not a conductive material, but is a magnetic material that has an electrical conductivity value of 8×10^{-4} S/cm [19].

Charge-Discharge Properties

The potential shown by the α -Fe₂O₃ sample is in the range between 9.98 and -9.98 V. The α -Fe_{1.94}Co_{0.06}O₃ sample produces a potential range of 3.64 and -4.76 V, while the sample of α -Fe_{1.92}Co_{0.08}O₃ shows a potential range that gets bigger as the cycles increase, which was originally in the range of 8.79 and -8.41 V for the first cycle changing in the 10th cycle to 9.98 V and -9.98 V. Sample α -Fe₂O₃ has the smallest current range, 5.5×10^{-4} A for the charge process and -3.3×10^{-4} A for discharge. The 0.0018 and 0.0027 mol doping samples have a relatively constant current range of 1×10^{-3} A and emit a current of -1×10^{-3} A. The sample that shows the presence of pairs of reduction and oxidation peaks is the hematite-Co 6%, indicating that the battery with this sample has α -Li_xFe_{1.92}Co_{0.08}O₃. The following is the charge-discharge reaction that takes place in a battery [20]:

Cathode (Positive electrode)



Anode (Negative electrode)

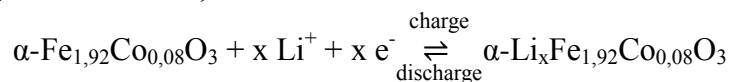


Table 1. The specific capacity of the samples synthesized using precipitation agents of NaOH and KOH

Sample	Specific capacity (mAh/g)			
	NaOH		KOH	
	Cycle 1	Cycle 10	Cycle 1	Cycle 10
$\alpha\text{-Fe}_2\text{O}_3$	1.30	1.30	0.03	0.02
$\alpha\text{-Fe}_{1.94}\text{Co}_{0.06}\text{O}_3$	1.84	0.70	1.84	1.84
$\alpha\text{-Fe}_{1.92}\text{Co}_{0.08}\text{O}_3$	1.14	0.77	1.84	1.84

On these three samples, it can be seen that giving cobalt doping to the samples synthesized using KOH, can increase the specific charge and discharge capacity. The $\alpha\text{-Fe}_{1.92}\text{Co}_{0.08}\text{O}_3$ sample produces the largest specific capacity, namely a charge of 1.85 mAh/g and a discharge of 1.84 mAh/g with a battery capacity efficiency of 99.9%. Meanwhile, samples synthesized using NaOH produce fluctuating specific capacity values, where the samples that show the best electrochemical performance are samples with 4% Co doping. In the first cycle, it was able to produce a discharge-specific capacity of 1.84 mAh/g with a voltage of -5.27 V and a charge of 2 mAh/g with a voltage of 4.77 V. The decrease in specific capacity was related to the crystal size, where the sample that was doped with cobalt using KOH had a smaller crystal size compared to samples without doping, the smaller the crystal size, the shorter the diffusion path for Li^+ ions to the anode [21]. In addition, this sample also shows the best electrochemical performance because the material is more stable. The decrease in charge and discharge capacity produced by samples with the NaOH precipitating agent is possible due to the formation of a solid electrolyte interface (SEI) layer that is too thick and does not decompose completely so that it can inhibit the intercalation process of Li^+ ions towards the anode [21]. Apart from that, a decrease in capacity can also be caused by the inability of the anode material to withstand volume changes during the redox process.

Conclusion

The synthesized precipitate obtained has a brick red and black color. FTIR analysis shows that the sample contains the Fe-O-Fe functional group which appears at wave numbers 519.19 and 517.32 cm^{-1} . Based on XRD characterization, it was found that the undoped sample had a crystal size of 26.4193 nm, while the 4% Co-doped sample was 20.6927 nm. SEM characterization results show that the morphology of the 6% Co-doped sample has an irregular semi-spherical shape. The battery with the best electrochemical performance is demonstrated by the 6% doping sample which has a conductivity value of 2.35×10^{-3} S/cm and a battery capacity efficiency of 99.9%.

Acknowledgements

Thank you to FSM UNDIP for providing funding for this research through DIPA FSM.

REFERENCES

1. Scrosati, B. and Garche, J. 2010, Lithium batteries: Status, prospects and future, *Journal of power sources*, **195**(9), 2419-2430
2. Wang, X., Qu, Q., Hou, Y., Wang, F., and Wu, Y., 2013, An aqueous rechargeable lithium battery of high energy density based on coated Li metal and LiCoO₂ *Chemical Communications*, **49**(55), 6179-6181
3. Subhan, A., Suwandi, E. and Ramlan, T. H. U., 2011, Efek Penambahan Bahan Aditif Mwcnt dan Acetylene Black (Ab) Pada Komposit Li₄Ti₅O₁₂ Sebagai Bahan Anoda Untuk Baterai Li-Ion. Departemen Teknik Metalurgi dan Material Universitas Indonesia, Jakarta
4. Liu, Y. and Yang, Y. 2016, Recent Progress of TiO₂-Based Anodes for Li-Ion Batteries, *Journal of Nanomaterials*
5. Fouad, D. E., Zhang, C., El-Didamony, H., Yingnan, L., Mekuria, T. D. and Shah, A. H. 2019, Improved size, morphology and crystallinity of hematite (α -Fe₂O₃) nanoparticles synthesized via the precipitation route using ferric sulfate precursor, *Results in Physics*, **12**, 1253-1261
6. Lassoued, A., Lassoued, M. S., Dkhil, B., Gadri, A., and Ammar, S., 2017, Synthesis, structural, optical and morphological characterization of hematite through the precipitation method: Effect of varying the nature of the base, *Journal of Molecular Structure*, **1141**, 99-106
7. Nithyadharseni, P., Abhilash, K., Petnikota, S., Anilkumar, M., Jose, R., Ozoemena, K., Vijayaraghavan, R., Kulkarni, P., Balakrishna, G. and Chowdari, B., 2017, Synthesis and lithium storage properties of Zn, Co and Mg-doped SnO₂ nanomaterials, *Electrochimica Acta*, **247**, 358-370
8. Wu, Z.-g., Zhong, Y.J., Liu, J., Wu, J.H., Guo, X.D., Zhong, B.-h. and Zhang, Z.Y., 2015, Subunits controlled synthesis of α -Fe₂O₃ multi-shelled core-shell microspheres and their effects on lithium/sodium ion battery performances, *Journal of Materials Chemistry A*, **3**(18), 10092-10099
9. Qi, X., Yan, Z., Liu, Y., Li, X., He, G. and Komarneni, S., 2018, Ni and Co doped yolk-shell type Fe₂O₃ hollow microspheres as anode materials for lithium-ion batteries, *Materials Chemistry and Physics*, **211**, 452-461
10. Harris, D. 2007. Ensiklopedi unsur-unsur kimia. Jakarta: Kawan Pustaka
11. Mansour, H., Letifi, H., Bargougui, R., De Almeida-Didry, S., Negulescu, B., Autret-Lambert, C., Gadri, A. and Ammar, S., 2017, Structural, optical, magnetic and electrical properties of hematite (α -Fe₂O₃) nanoparticles synthesized by two methods: polyol and precipitation, *Applied Physics A*, **123**(12), 787
12. Anggraini, T. 2017, Sintesis dan Karakteristik Fe_{2-x}La_xTiO sebagai Absorber Gelombang Elektromagnetik, *Skripsi*, Universitas Islam Negeri Syarif Hidayatullah, Jakarta
13. Popov, N., Bošković, M., Perović, M., Németh, Z., Wang, J., Kuang, Z., Reissner, M., Kuzmann, E., Homonnay, Z. and Kabuki, S., 2021, Influence of low-spin Co³⁺ for high-spin Fe³⁺ substitution on the structural, magnetic, optical and catalytic properties of hematite (α -Fe₂O₃) nanorods, *Journal of Physics and Chemistry of Solids*, **152**, 109929
14. Greenwood, N. and Earnshaw, A. 1997, Chemistry of the Elements, 2nd Edition, Butterworth-Heinemann, Oxford
15. Gerth, J. 1990, Unit-cell dimensions of pure and trace metal-associated goethites, *Geochimica et Cosmochimica Acta*, **54**(2), 363-371
16. Pozas, R., Rojas, T. C., Ocaña, M. and Serna, C. J., 2004, The nature of Co in synthetic Co-substituted goethites, *Clays and Clay Minerals*, **52**(6), 760-766
17. Alvarez, M., Sileo, E. E. and Rueda, E. H., 2008, Structure and reactivity of synthetic Co-substituted goethites, *American Mineralogist*, **93**(4), 584-590
18. Novialent, E. 2018. Pengaruh variasi doping Ni terhadap mikrostruktur dan konduktivitas material katoda LiNi_xFe_{1-x}PO₄. Institut Teknologi Sepuluh Nopember: Surabaya
19. Purwanto, P. and Kusumawati, D. H. 2013, Karakterisasi Sifat Listrik dan Magnetik PANI/HCl/Fe₃O₄ akibat Penambahan Fe₃O₄ pada Komposit PANI/HCl, *Sains & Matematika*, **2**(1), 2302-7290
20. Xiong, S. 2019, A study of the factors that affect lithium ion battery degradation, University of Missouri-Columbia, Columbia
21. Permana, G. A. 2016, Analisa Pengaruh Konsentrasi NH₄Br pada Proses Sintesa Anoda MnO₂ Terhadap Morfologi dan Performa Elektrokimia Baterai Lithium Ion, Institut Teknologi Sepuluh Nopember: Surabaya